

## THE VARIATION OF PROFILE OF $\gamma$ -STAINLESS STEEL WELD BEAD WITH A CHANGE OF HEAT INPUT

Manas Kumar Saha<sup>1</sup>, Lakshmi Narayan Dhara<sup>2</sup> and Santanu Das<sup>3\*</sup>

Mechanical Engineering Department, Kalyani Govt. Engineering College, Kalyani- 741235, West Bengal, India

<sup>1</sup>Presently working as Lecturer, Engineering Institute for Junior Executives, Dalalpur, Howrah-711104, West Bengal, India. \*Corresponding author

Email: <sup>1</sup>manassaha71@gmail.com, <sup>2</sup>Indhara93@gmail.com, <sup>3</sup>sdas.me@gmail.com

Paper received on : 19/10/2018, accepted after revision on : 20/05/2019

DOI : 10.21843/reas/2017/46-56/184053

**Abstract :** Cladding is usually done to protect a surface from corrosive or erosive wearing. Better cladding demands optimum weld bead geometry that should have less penetration giving less dilution. Heat input plays a vital role to produce a weld bead profile characterized by its width, reinforcement and depth of penetration and some shape factors like RFF (reinforcement form factor) and PSF (penetration shape factor). In the present case, 316 austenitic stainless steel bead was produced on E250 low alloy steel by GMAW process using only carbon dioxide as the shielding gas. Nine bead-on-plate samples were produced with nine different heat inputs. Welding voltage was kept constant. Experiments were replicated twice for achieving more reliability. Experimental results showed that width, height and depth of weld bead got larger with larger heat input on the whole. On the contrary, shape factors like reinforcement form factor and penetration shape factor tend to become smaller with larger heat input. Linear regression analysis is carried out to evaluate the relation between heat input and different bead profile components as well as shape factors. ANOVA table suggests the equations proposed by regression analysis are explainable and significant at 95% significant level.

**Keyword:** Cladding, welding, bead-on-plate, weld bead geometry, regression analysis.

### 1. INTRODUCTION

Cladding is a surfacing technique of depositing few millimeters of superior materials having better corrosion and erosion resistance property along with mechanical strength onto low grade base material by means of coalescence with or without application of heat and pressure. Quality of cladding largely depends on composition of both of cladding and base materials, process parameters, bead geometry, etc. Various arc welding processes, rolling, explosive welding, resistance welding, hybrid welding, etc. can be used to produce cladding [1].

Gas metal arc welding is a semiautomatic, user-friendly, cost effective and versatile method that are popularly used to producing cladding [2]. GMAW process uses 100% CO<sub>2</sub> as shielding gas it is called as metal active gas welding. It is further cost effective but yields considerable amount of spatter. The drawbacks of MAG welding can be minimized by selecting process parameters at a proper level [3].

Different grades of stainless steels such as austenitic stainless steel [4], duplex stainless steel [5-7], super duplex stainless steel, etc. are used as cladding layer due to their

improved corrosion resistance properties as well as better mechanical properties. Austenitic stainless steel is a relatively low cost cladding material and shows moderate corrosion resistance in chloride atmosphere [8].

Weld bead geometry takes an important role in cladding as well as welding performance. Unlike welding, cladding demands wider weld bead, larger bead height and low bead depth to minimize dilution. Heat input is responsible for creating admissible weld bead profile. Process parameters like welding current, voltage and arc travel speed of electrode work together to control heat input and thus control profile of weld bead a lot. Several works have been carried out to evaluate favourable profile of weld bead made by different stainless steels is such as austenitic stainless steel, duplex stainless steel, etc. on low alloy steel or even mild steel with the help of gas metal arc welding, submerged arc welding, gas tungsten arc welding, laser arc welding, etc. Different statistical tools/mathematical models such as regression analysis [9], RSM [10], different neural network [11], analytical hierarchy method [12-13], Taguchi method [14], etc. have been used to establish relationship among process parameters and weld bead profile elements such as bead width (W), bead height (R), bead depth (P) and some ratios such as reinforcement form factor (RFF, ratio of W to R), penetration shape factor (PSF, ratio of W to P), etc. In one earlier

experiment, Saha et al. observed that all components of weld bead profile as well as shape factors accumulate with spurting heat input for duplex stainless steel weld bead on low alloy constructional steel by flux-cored arc welding process using only CO<sub>2</sub> as shielding gas [15]. In another work, Saha et al. observed bead width, RFF and PSF change in direct proportion to heat input for austenitic stainless steel weld bead formed on low alloy constructional steel by metal active gas welding process [16].

In ongoing investigation, duplex stainless steel (E2209 T01) weld beads were made on low alloy constructional steel (E350) by gas metal arc welding using carbon di oxide as shielding gas. Heat input (Q) for welding was varied by varying welding current and electrode travel speed at three levels each, keeping welding voltage constant throughout the experiment. Visual inspection and the macrostructure study of nine weld beads were performed. Experimental results are analyzed by regression analysis method to evaluate linear relation between each of W, R, P, RFF, PSF with Q at as high as 95% confidence level.

## 2. EXPERIMENTAL PROCEDURE

### 2.1. Base material

Low alloy constructional steel E250 is used as base material for the experiment. The chemical composition is shown in Table 1.

**Table 1:** Chemical composition of E250 grade low alloy constructional steel

|       |       |        |       |       |          |        |
|-------|-------|--------|-------|-------|----------|--------|
| Wt.%C | Wt%Si | Wt%Mn  | Wt%P  | Wt%S  | Wt%Cr    | Wt%Al  |
| 0.19  | 0.14  | 0.49   | 0.06  | 0.03  | <0.001   | 0.0003 |
| Wt%Ni | Wt%Co | Wt%Cu  | Wt%Nb | Wt%Ti | Wt%V     | Wt%Sn  |
| 0.025 | 0.006 | 0.005  | 0.009 | 0.002 | 0.002    | 0.014  |
| Wt%Pb | Wt%As | Wt%Zn  | Wt%B  | Wt%Zr | Wt%Fe    |        |
| 0.013 | 0.066 | <0.001 | 0.001 | 0.002 | <98.8810 |        |

Carbon equivalent of the base metal is nearly,  $C_{eq} = 0.235$

**Table 2:** Chemical composition of austenitic stainless steel

|       |        |       |       |        |        |       |
|-------|--------|-------|-------|--------|--------|-------|
| Wt%C  | Wt%Si  | Wt%Mn | Wt%P  | Wt%S   | Wt%Cr  | Wt%Mo |
| 0.076 | 0.182  | 1.102 | 0.028 | 0.008  | 15.046 | 2.091 |
| Wt%Ni | Wt%Al  | Wt%Co | Wt%Cu | Wt%Nb  | Wt%Ti  | Wt%V  |
| 9.937 | 0.0105 | 0.074 | 0.342 | 0.002  | 0.0316 | 0.048 |
| Wt%W  | Wt%Sn  | Wt%Ce | Wt%B  | Wt%Fe  |        |       |
| 0.026 | 0.0103 | 0.010 | 0.001 | <70.95 |        |       |

Carbon equivalent of filler electrode is nearly,  $C_{eq} = 4.38$

## 2.2. Electrode

Austenitic stainless steel of grade 316 was used to produce weld bead on E250 base metal. The chemical composition of austenitic stainless steel is shown in Table 2.

## 2.3. Welding technique

Gas metal arc welding using full of CO<sub>2</sub> as shielding gas was used to produce weld bead. Thus the welding process is renowned as metal active gas welding or MAG welding. Gas flow rate was constant and it was 16 lit/min.

## 2.4. Welding equipment

GMAW machine (Model: Auto k 400) was used for the experiment made by ESAB India Ltd.

## 2.5. Welding procedure

Welding gun was attached with a motor operated vehicle by one fixture guided by a fixture containing rails. Angle of electrode, electrode tip-workpiece distance, gas flow rate and movement of electrode torch were kept constant for a particular specimen. Change of speed of electrode was maintain-

ed by motor which was actually controlled by a variac.

## 2.6. Process parameters

Heat input is taken as the most important parameter for weld bead geometry formation. Heat input varies with change in process parameters like welding current, torch travel speed and welding voltage theoretically. Heat input measured theoretically by the help of equation (1).

$$Q = \frac{\text{Voltage} \times \text{current} \times 60}{\text{Travel sprrd} \times 1000} \times \eta \quad (1)$$

Where,

'Q' is Heat Input in kJ/mm, 'Travel Speed' is expressed in mm/min, 'η' represents Efficiency (In this experiment, it is taken as 0.8).

In the present work, welding current and arc travel speed are selected in three levels, keeping welding voltage constant. Nine weld beads were prepared applying different heat inputs produced by these parameters. The whole work was done twice for better reliability. Table 3 shows parameter combinations used in the present work.

**Table 3:** Heat input and other process parameters of cladding

| Sample number | Welding Current, I (A) | Arc Travel Speed, S (mm/min) | Welding Voltage (V) | Heat Input, Q (kJ/mm) |
|---------------|------------------------|------------------------------|---------------------|-----------------------|
| 1             | 140                    | 360                          | 27                  | 0.504                 |
| 2             | 140                    | 390                          | 27                  | 0.465                 |
| 3             | 140                    | 420                          | 27                  | 0.434                 |
| 4             | 170                    | 360                          | 27                  | 0.612                 |
| 5             | 170                    | 390                          | 27                  | 0.564                 |
| 6             | 170                    | 420                          | 27                  | 0.524                 |
| 7             | 200                    | 360                          | 27                  | 0.720                 |
| 8             | 200                    | 390                          | 27                  | 0.664                 |
| 9             | 200                    | 420                          | 27                  | 0.617                 |

### 2.7. Specimen preparation

Specimens were produced by cutting the bead-on-plate transversely and finished by grinding and polishing by emery belt and

polishing disc subsequently. The finished surface was then etched by 2% nital solution. Fig. 1 and Fig. 2 represent front and top view of all the specimens.



**Fig. 1:** Front view of bead profile of all specimens



**Fig. 2:** Top view of weld beads on workpieces.

**2.8. Visual observation of bead-on-plate experiments**

Observations with naked eye was done to obtain weld defects like spatter, undercut, etc. and nature of weld bead like whether it was continuous, smooth, etc. or not.

**2.9. Observation of weld bead profile**

Polished specimens were etched by 2% nital solution and were observed under Tool Makers' Microscope. Bead profile parameters like width, depth and height of weld bead were determined by the help of a scale inside the microscope.

**3. RESULTS AND DISCUSSION**

Visual inspection indicates the results that

are shown in Table 4. Results obtained from observation of weld bead profile are shown in Table 5 and 6. Results obtained from 1st set and 2nd set of experiment are shown in table number 5 and 6 respectively.

From the results obtained by visual inspection, it was observed that spatters were presented in moderate to high quantity on the weld beads and their surroundings due to use of CO<sub>2</sub> as shielding gas. The amount of spatter decreased as the heat input increased. It was also observed that spatters were decreased with an increase in current and decrease in travel speed of the filler electrode, keeping voltage constant.

**Table 4:** Results obtained from naked eye observation of bead formed on plate

| Sl. No. | Sam ple No.    | (V) | I(A) | S <sub>v</sub> (mm/min) | Q <sub>v</sub> (kJ/mm) | Blow hole/ undercut |                  | Continuity in deposition |                  | Spatter          |                  |
|---------|----------------|-----|------|-------------------------|------------------------|---------------------|------------------|--------------------------|------------------|------------------|------------------|
|         |                |     |      |                         |                        | 1st Repli cation    | 2nd Repli cation | 1st Repli cation         | 2nd Repli cation | 1st Repli cation | 2nd Repli cation |
| 1       | S <sub>7</sub> | 27  | 140  | 420                     | 0.434                  | Nil                 | Nil              | Cont.                    | Cont.            | high             | Med.             |
| 2       | S <sub>2</sub> | 27  | 140  | 390                     | 0.465                  | Nil                 | Nil              | Cont.                    | Cont.            | High             | Med.             |
| 3       | S <sub>1</sub> | 27  | 140  | 360                     | 0.504                  | Nil                 | Nil              | Cont.                    | Cont.            | Med.             | Med.             |
| 4       | S <sub>6</sub> | 27  | 170  | 420                     | 0.524                  | Nil                 | Nil              | Cont.                    | Cont.            | Low              | Med.             |
| 5       | S <sub>5</sub> | 27  | 170  | 390                     | 0.564                  | Nil                 | Nil              | Cont.                    | Cont.            | High             | High             |
| 6       | S <sub>4</sub> | 27  | 170  | 360                     | 0.612                  | Nil                 | Nil              | Cont.                    | Cont.            | Med.             | Med.             |
| 7       | S <sub>9</sub> | 27  | 200  | 420                     | 0.617                  | Nil                 | Nil              | Cont.                    | Cont.            | Low              | Med.             |
| 8       | S <sub>8</sub> | 27  | 200  | 390                     | 0.664                  | Nil                 | Nil              | Cont.                    | Cont.            | Med.             | Med.             |
| 9       | S <sub>7</sub> | 27  | 200  | 360                     | 0.720                  | Nil                 | Nil              | Cont.                    | Cont.            | Low              | Med.             |

Cont. = continuous, Med. = medium,

**Table 5:** Values of weld bead profile elements from first set of bead formed on plate

| Specimen No.   | (V)<br>(Volt) | (I)<br>(A) | (S)<br>(mm/min) | Q<br>(kJ/mm) | Weld bead width<br>(W)<br>(mm) | Bead height<br>(R)<br>(mm) | Depth of bead<br>(P)<br>(mm) | PSF=(W/P) | RFF=(W/R) |
|----------------|---------------|------------|-----------------|--------------|--------------------------------|----------------------------|------------------------------|-----------|-----------|
| S <sub>3</sub> | 27            | 140        | 420             | 0.434        | 5.000                          | 1.950                      | 1.650                        | 3.030     | 2.564     |
| S <sub>2</sub> | 27            | 140        | 390             | 0.465        | 5.500                          | 2.250                      | 1.900                        | 2.894     | 2.444     |
| S <sub>1</sub> | 27            | 140        | 360             | 0.504        | 5.680                          | 2.450                      | 2.100                        | 2.704     | 2.318     |
| S <sub>6</sub> | 27            | 170        | 420             | 0.524        | 5.755                          | 2.615                      | 1.040                        | 5.533     | 2.200     |
| S <sub>5</sub> | 27            | 170        | 390             | 0.564        | 5.900                          | 2.745                      | 1.400                        | 4.214     | 2.149     |
| S <sub>4</sub> | 27            | 170        | 360             | 0.612        | 5.855                          | 2.585                      | 1.425                        | 4.108     | 2.264     |
| S <sub>9</sub> | 27            | 200        | 420             | 0.617        | 6.005                          | 2.500                      | 1.500                        | 4.003     | 2.402     |
| S <sub>8</sub> | 27            | 200        | 390             | 0.664        | 6.060                          | 2.800                      | 1.790                        | 3.385     | 2.164     |
| S <sub>7</sub> | 27            | 200        | 360             | 0.720        | 6.500                          | 3.135                      | 2.490                        | 2.610     | 2.073     |

**Table 6:** Values of weld bead geometry components from second set of bead formed on plate

| Specimen No.                | (V)<br>(Volt) | (I)<br>(A) | (S)<br>(mm/min) | Q<br>(kJ/mm) | Bead width<br>(W)<br>(mm) | Bead height<br>(R)<br>(mm) | Depth of bead<br>(P)<br>(mm) | PSF=(W/P) | RFF=(W/R) |
|-----------------------------|---------------|------------|-----------------|--------------|---------------------------|----------------------------|------------------------------|-----------|-----------|
| S <sub>3</sub> <sup>*</sup> | 27            | 140        | 420             | 0.434        | 5.125                     | 1.875                      | 1.425                        | 3.596     | 2.733     |
| S <sub>2</sub> <sup>*</sup> | 27            | 140        | 390             | 0.465        | 5.620                     | 2.000                      | 1.685                        | 3.335     | 2.810     |
| S <sub>1</sub> <sup>*</sup> | 27            | 140        | 360             | 0.504        | 5.995                     | 2.125                      | 1.715                        | 3.472     | 2.821     |
| S <sub>6</sub> <sup>*</sup> | 27            | 170        | 420             | 0.524        | 5.775                     | 2.525                      | 1.325                        | 4.358     | 2.287     |
| S <sub>5</sub> <sup>*</sup> | 27            | 170        | 390             | 0.564        | 5.650                     | 2.415                      | 1.500                        | 3.766     | 2.339     |
| S <sub>4</sub> <sup>*</sup> | 27            | 170        | 360             | 0.612        | 6.000                     | 2.500                      | 1.840                        | 3.260     | 2.400     |
| S <sub>9</sub> <sup>*</sup> | 27            | 200        | 420             | 0.617        | 6.350                     | 2.952                      | 1.800                        | 3.527     | 2.151     |
| S <sub>8</sub> <sup>*</sup> | 27            | 200        | 390             | 0.664        | 6.550                     | 2.685                      | 1.755                        | 3.732     | 2.439     |
| S <sub>7</sub> <sup>*</sup> | 27            | 200        | 360             | 0.720        | 6.700                     | 2.750                      | 2.050                        | 3.268     | 2.436     |

Different plots are developed using results obtained from macrostructure analysis of two replicated experiments. The plots are prepared by using average values of two experimental results, showing the higher and

lower value by means of bar for each value. Fig. 1 through Fig. 5 show scatter plots that represent variation of width, height, depth of weld bead as well as RFF and PSF with heat input respectively.

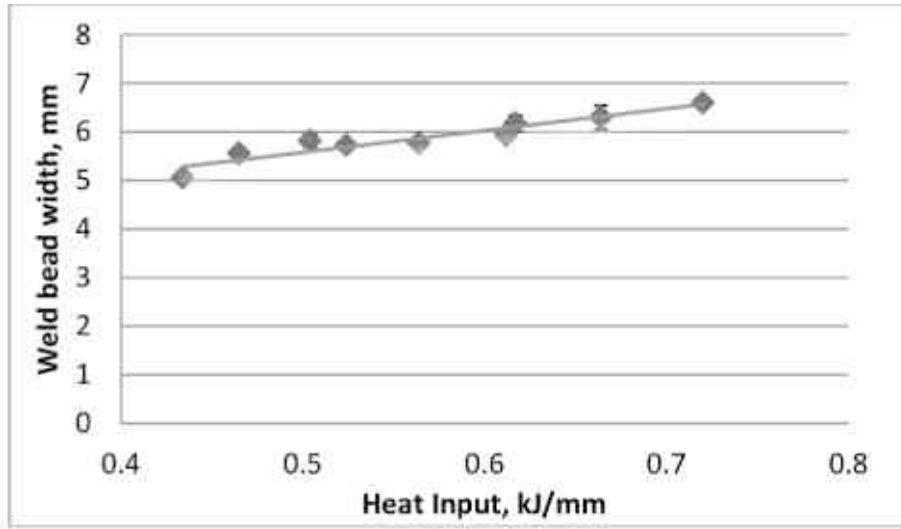


**Fig.3:** Plot of variation of weld bead width with heat input as obtained from 1st and 2nd set of experiments

From Fig. 3, it can be observed clearly that weld bead (W) widens with increasing heat input almost linearly. Increased molten metal formed at higher heat input may be the cause of wider weld bead.

Fig. 4 represents change in bead height against change in heat input. The plot shows clear cut increase in bead height against increasing heat input. Highest bead height is achieved at maximum heat input used in this work.

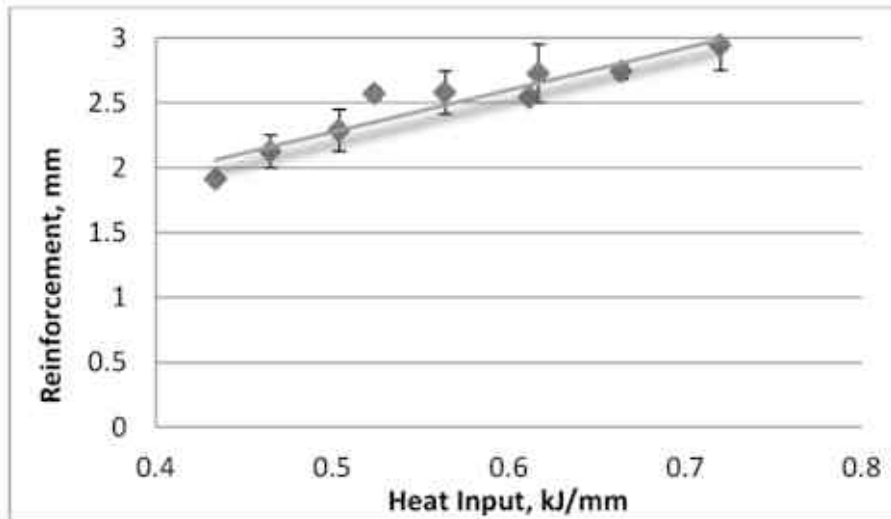


**Fig.4:** Plot of variation of reinforcement with heat input as obtained from 1st and 2nd set of experiments

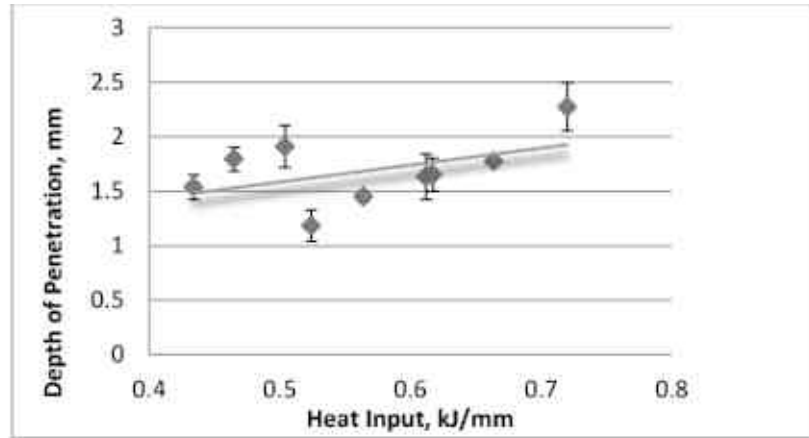


**Fig.5:** Plot of change of bead depth with heat input as obtained from 1st and 2nd set of experiments

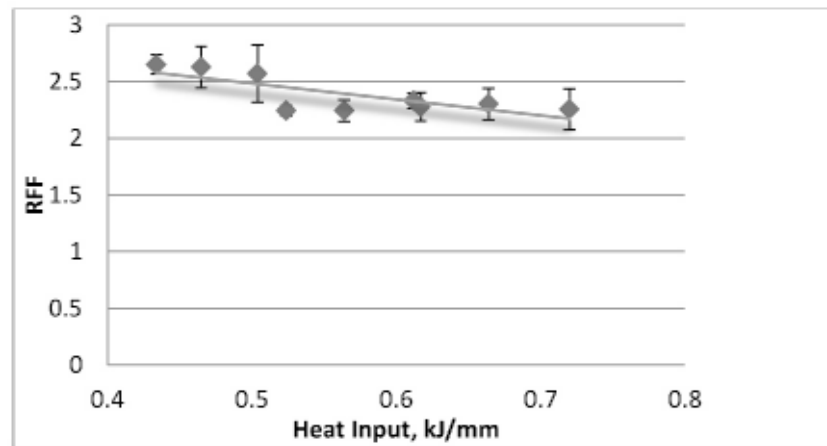


**Fig.6:** Plot of change of RFF with heat input as obtained from 1st and 2nd set of experiments

Fig.5 depicts the tendency of depth of penetration against increasing heat input. An overall increasing tendency of depth of penetration with some deviation is observed with increase in heat input. In fact, first depth inclines with inclination of heat input up to 0.504 kJ/mm and then declines sharply at 0.524 kJ/mm heat input. Bead depth increases further nearly in linear pattern and

gets its maximum value at the highest heat input considered in this experiment.

Fig.6 shows the change in RFF values with gradually larger heat input. Although there is no appreciable variation in the value of RFF, an overall decrease in RFF is observed as heat input gets higher values.

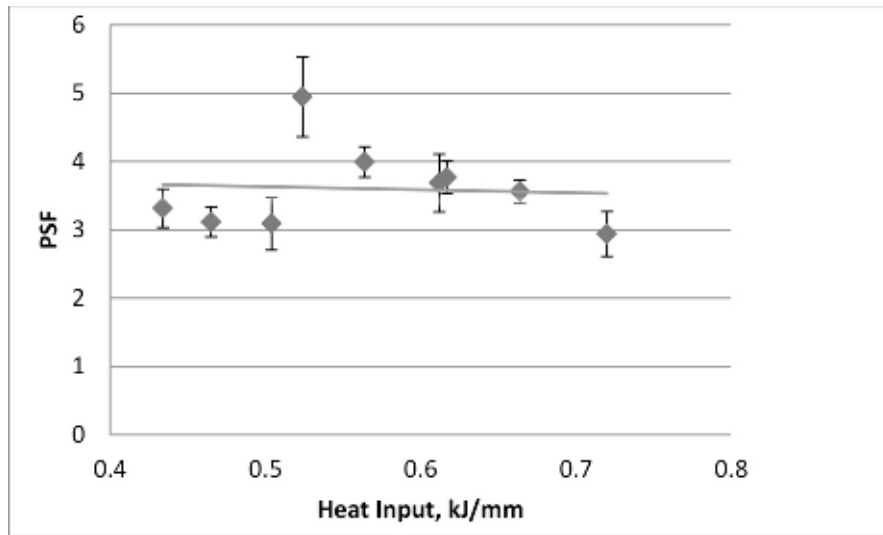


**Fig.7:** Plot of variation of PSF with heat input as obtained from 1st and 2nd replications

Fig.7 shows the change in PSF with change in heat input. On the whole, there is no much noticeable variation in the value of PSF. However, at around 0.5 kJ/mm heat input, there is a large variation in PSF. The reason behind could not be ascertained yet.

From different plots, it can be stated that width and height of weld bead become larger clearly with higher heat input. Bead depth increases with larger heat input broadly, though some deviation is also found. But, RFF decreases slightly with larger heat input. PSF does not indicate clear trend related to heat input.

**4. REGRESSION ANALYSIS**

Regression analysis is employed to obtain

relationship between heat input and bead profile elements statistically. Relation between width, depth and height of weld bead in connection with heat input are shown by equation (2) to (4).

$$\text{Beadwidth}(W) = 4.467 * Q + 3.359 \quad (2)$$

$$\text{Bead depth}(P) = 1.368953 * Q + 0.923096 \quad (3)$$

$$\text{Bead height}(R) = 1.548 * Q + 0.8097 \quad (4)$$

ANOVA Tables suggest that these equations are significant at 95% confidence level. ANOVA tables for weld bead with heat input, reinforcement height with heat input and depth of penetration with heat input are given in Table 7, Table 8 and Table 9 respectively.

**Table 7:** Analysis of Variance for regression equation between bead width and heat input

| Source     | DF | SS             | MS      | F     | P     |
|------------|----|----------------|---------|-------|-------|
| Regression | 1  | 1.42222        | 1.42222 | 58.31 | 0.000 |
| Error      | 7  | 0.17073        | 0.02439 |       |       |
| Total      | 8  | 1.59296        |         |       |       |
|            |    | $R^2 = 89.3\%$ |         |       |       |

**Table 8:** Analysis of Variance for regression equation between bead height and heat input

| Source         | DF | SS       | MS       | F    | P     |
|----------------|----|----------|----------|------|-------|
| Regression     | 1  | 0.518542 | 0.518542 | 8.98 | 0.020 |
| Error          | 7  | 0.404347 | 0.057764 |      |       |
| Total          | 8  | 0.922889 |          |      |       |
| $R^2 = 56.2\%$ |    |          |          |      |       |

**Table 9:** Analysis of Variance for regression equation between bead depth and heat input

| Source         | DF | SS       | MS       | F    | P     |
|----------------|----|----------|----------|------|-------|
| Regression     | 1  | 0.170852 | 0.170852 | 2.08 | 0.193 |
| Error          | 7  | 0.575704 | 0.082243 |      |       |
| Total          | 8  | 0.746556 |          |      |       |
| $R^2 = 22.9\%$ |    |          |          |      |       |

Table 7 expresses value of  $R_2$  for the linear regression equation (2) to be 89.3% which signifies strong relationship between W and Q is been establish. The Table also very low value of P and high value of F which signifies greater chance of occurring bead width with change in heat input obeying the equation.

The moderate value of  $R_2$  obtained from Table 8 depicts moderate relationship between bead height and heat input. Moderately high value of P and moderately low value of F represents moderate chance for obeying equation (3) relating reinforcement height to a particular value of Q.

Quite less value of  $R^2$  obtained from Table 9 shows weak relationship between P and Q. The high value of P and less value of F also agree with less chance of occurrence of the depth of penetration against certain value of Q obeying equation (4). Wide deviation in data in Fig. 5 supports this relation.

No such relationship between PSF and RFF with heat input is tried to develop as there are remarkable scatterings of data as seen in Fig.6 and Fig.7.

## 5. CONCLUSION

Observing the results from the experimensts done, it may be concluded that :

- ❖ Heat input influences bead geometry components as higher heat input causes higher volume of molten weld pool.
- ❖ Width, depth, height of weld bead profile increase with increase in heat input on the whole, when weld bead width and reinforcement height are found to be mostly influenced by heat input within the experimental domain.

## REFERENCES

- [1] Saha, M.K. and Das, S., Gas Metal Arc Weld Cladding and its Anti-Corrosive Performance- A Brief Review, Athens Journal of Technology and Engineering, Vol.5, No.1, pp.155-174, 2018.
- [2] Conon, L.P., Welding Hand Book, 8th Edition, Vol. 1, American Welding Society, USA, 1987.
- [3] Saha, M.K. and Das, S., A Review on Different Cladding Techniques Employed

- to Resist Corrosion, Journal of the Association of Engineers, India, Vol. 86, No. 1 & 2, pp.51-63, 2016. DOI: 10.22485/jaei/2016/v86/i1-2/11984
- [4] Verma, A.K., Biswas, B.C., Roy, P., De, S., Saren, S. and Das, S., Exploring Quality of Austenitic Stainless Steel Clad Layer Obtained by Metal Active Gas Welding, Indian Science Cruiser, Vol.27(4), pp.24-29, 2013.
- [5] Kannan, T. and Muguran, N., Effect of Flux Cored Arc Welding Process Parameters on Duplex Stainless Steel Clad Quality, J. of Mat. Proc. Tech., Vol.176, pp.230-239, 2006.
- [6] Verma, A.K., Biswas, B.C., Roy, P., De, S., Saren, S. and Das, S., On the effectiveness of duplex stainless steel cladding deposited by gas metal arc welding, e-proc. 67th Int. Conf. of Annual Assembly of the Int. Inst. of Welding, Seoul, Korea, 2014.
- [7] Chakraborty, B., Das, H., Das, S. and Pal, T.K., Effect of process parameters on clad quality of duplex stainless steel using GMAW process, Trans. of Ind. Inst. of Metals, Vol.66(3), pp.221-230, 2013.
- [8] Khara, B., Mandal, N.D., Sarkar, A., Sarkar, M., Chakrabarti, B. and Das, S., Weld cladding with austenitic stainless steel for imparting corrosion resistance, Indian Welding Journal, Vol.49(1), pp.75-81, 2016.
- [9] Xiong, J., Zhang, G., Hu, J. and Wu, L., Bead geometry prediction for robotic GMAW-based rapid manufacturing through a neural network and a second-order regression analysis, Journal of Intellectual Manufacturing, Vol.25, pp 157-163, 2014. DOI: 10.1007/s10845-012-0682-1
- [10] Jayachandrana, J.A.R. and Murugan, N., Investigations on the Influence of Surfacing Process Parameters over Bead Properties during Stainless Steel Cladding, Materials and Manufacturing Processes, Vol.27, pp.69-77, 2012.
- [11] Datta, S., Bandyopadhyay, A. and Pal, P.K., Grey-based Taguchi method for optimization of bead geometry in submerged arc bead-on-plate welding. The International Journal of Advanced Manufacturing Technology, Vol.39, No.11, pp.1136-1143, 2008. DOI: 10.1007/s00170-007-1283-6.
- [12] Sabiruddin, K., Das, S. and Bhattacharya, A., Application of Analytical Hierarchy Process for Optimization of Process Parameters in GMAW, Indian Welding Journal, Vol.42(1), pp.38-46, 2009.
- [13] Sabiruddin, K., Bhattacharya, S. and Das, S., Selection of Appropriate Process Parameters for Gas Metal Arc Welding of Medium Carbon Steel Specimens, Int. J. for Analytical Hierarchy Process, Vol.5, pp.252-266, 2013.
- [14] Sarkar, A. and Das, S., Application of Grey-based Taguchi Method for Optimizing Gas Metal Arc Welding of Stainless Steel, Indian Welding Journal, Vol.44, pp.37-48, 2011.
- [15] Mondal, A., Saha, M.K., Hazra, R. and Das, S., Influence of Heat Input on Weld Bead Geometry Using Duplex Stainless Steel Wire Electrode on Low Alloy Steel Specimens, Cogent Engineering, Vol.3, No.1, pp.1143598/1-14, 2016.
- [16] Saha, M.K., Hazra, R., Mondal, A. and Das S., Effect of Heat Input on Geometry of Austenitic Stainless Steel Weld Bead on Low Carbon Steel, Journal of The Institution of Engineers (India), Series C, 2018. DOI 10.1007/s40032-018-0461-7.